J Mammal Evol (2016) 23:337–352
DOI 10.1007/s10914-016-9327-z

ORIGINAL PAPER

The inner ear of *Protungulatum* (Pan-Euungulata, Mammalia)

M. J. Orliac[1] · **M. A. O'Leary**[2]

Published online: 4 April 2016

Abstract We present new anatomical details about the bony labyrinth of *Protungulatum* based on micro CT-scan investigation of an isolated petrosal bone retrieved at the Puercan locality of Bug Creek Anthills and referred to *Protungulatum* sp. The exceptional state of preservation of the specimen allowed us to reconstruct the very fine details of the inside of the petrosal bone, including the bony labyrinth, the innervation of the vestibule and the innervation and vasculature of the cochlea. Estimation of the auditory capability of *Protungulatum* based on cochlear morphology indicate that *Protungulatum* was specialized for high-frequency hearing, with estimated low frequency limits above 1 KHz. Comparisons with Late Cretaceous non-placental eutherians and with early Tertiary pan-euungulates indicate that the bony labyrinth of *Protungulatum* is closer in general morphology to Mesozoic forms (low coiling and low aspect ratio of the cochlea, posterior orientation of the common crus, dorsal outpocketing of the cochlear fossula), and shares only a few characters with pan-euungulate and euungulate taxa. Interestingly, the bony labyrinth of *Protungulatum* also shares some morphological features with South American notoungulates and litopterns recently described from Itaboraí, Brazil. These new observations provide new morphological features of potential phylogenetic interest.

Keywords Bony labyrinth · "Condylarthra" · Vestibulocochlear nerve · Spiral modiolar artery · Placentalia · Puercan · Bug Creek

Introduction

The petrosal bone of the ear region has been a rich source of comparative anatomical data for the last century and continues to play a key role in modern mammalian phylogenetics (e.g., Cifelli 1982; Novacek 1986; Wible 1990; MacPhee 1994; Wible et al. 1995, 2001; Rougier and Wible 2006; O'Leary 2010; Orliac 2013; Benoit et al. 2013). The petrosal is the bony housing for the organs of hearing and balance, behaviors that vary greatly among mammals. The petrosal bone frequently shows anatomical variation, but most comparative studies have concentrated on the variation of its external surface. However, the anatomy of the bony labyrinth housed within the petrosal presents a completely different suite of variable characters for comparative anatomy. These have not been easy to access before the widespread use of high quality micro-CT (computed tomography) scans. With this new imaging technique, our knowledge of the inner ear morphology of placental mammals has increased dramatically in recent decades (e.g., Ekdale 2009, 2013; Billet et al. 2012, 2015; Orliac et al. 2012; Macrini et al. 2013; Ravel and Orliac 2015), and detailed anatomical features of the bony labyrinth have begun to be integrated into phylogenetic studies (e.g., Ekdale et al. 2004; Lebrun et al. 2010; Benoit et al. 2013; Macrini et al. 2013). Here, we contribute to this growing body of knowledge with further descriptions of the inner ear of an extinct early placental mammal.

Electronic supplementary material The online version of this article (doi:10.1007/s10914-016-9327-z) contains supplementary material, which is available to authorized users.

✉ M. J. Orliac
maeva.orliac@univ-montp2.fr

[1] Institut des Sciences de l'Evolution, UMR 5554 CNRS, IRD, EPHE, Université de Montpellier, Place Eugène Bataillon, 34095 Montpellier, Cedex 5, France

[2] Department of Anatomical Sciences, HSC-T-8 (040), Stony Brook University, Stony Brook, NY 11794-8081, USA

The early diverging member of Pan-Euungulata (i.e., the clade uniting all taxa more closely related to crown euungulates than to any other extant taxon of placentals, O'Leary et al. 2013: supplementary materials) *Protungulatum* represents one of the earliest occurrences in the fossil record of a member of the crown clade Placentalia (O'Leary et al. 2013), and, therefore, by extension, also represents the earliest record of Pan-Euungulata. *Protungulatum* is documented by very scarce cranial remains (Sloan and Van Valen 1965; Wible et al. 2009; O'Leary 2010), and cranial characters for *Protungulatum* are mainly known from the morphology of the dentary and the external morphology of the petrosal bone (Sloan and Van Valen 1965; Wible et al. 2009; O'Leary 2010). We present new anatomical details regarding the bony labyrinth of *Protungulatum* based on a micro CT-scan investigation of an isolated petrosal bone (AMNH-VP 118359) retrieved at the Bug Creek Anthills locality, Montana (early Paleocene, Smit and Van der Kaars 1984). The exceptional state of preservation of the specimen allowed us to reconstruct very fine detail of the internal aspect of the petrosal bone including the bony labyrinth and the innervation of the vestibule and the innervation and vasculature of the cochlea.

Materials and Methods

Specimens

The internal structure of the petrosal described here is based on AMNH-VP 118359, a specimen from the Bug Creek Anthills locality of northeastern Montana (Sloan and Van Valen 1965). The taxonomy of the Bug Creek specimens has had a complicated history because individual anatomical elements from the locality are not typically associated with other elements, and AMNH-VP 118359 is no exception. MacIntyre (1972:286-287, figs: 4-5) described and figured the external anatomy of a Bug Creek petrosal that he called of a ""Ferungulate" variety." He did not supply specimen numbers and it is not clear whether his ferungulate illustration describes a composite or an individual specimen. MacIntyre (1972:297-298) suggested that the five ferungulate-type petrosals he identified might be affiliated with *Protungulatum*, a taxon known from dental remains at the same locality. Wible et al. (2009: appendix 1) listed MacIntyre (1972) as a source of data for the terminal taxon *Protungulatum* in their matrix. The Wible et al. (2009) matrix contains petrosal scores for *Protungulatum* (see also MorphoBank Project 316), scores that have to be based entirely on the MacIntyre (1972) paper because no other petrosal material of this taxon has been published (and no additional specimen numbers were listed in their appendix). Thus, Wible et al. (2009) followed the attribution of the MacIntyre (1972) ferungulate material to *Protungulatum* but provided no further justification or specimen numbers. AMNH -VP 118359 very closely resembles the morphology of the MacIntyre (1972) figure (see our discussion below). Based on this comparative anatomy, O'Leary (2010) referred AMNH -VP 118359 to *Protungulatum* sp.

Comparisons are made here with: (i) Late Cretaceous eutherians: *Kulbeckia kulbecke* (Ekdale and Rowe 2011: fig. 6; Ekdale 2013: fig. 6), zhelestids (URBAC 03–39; Ekdale 2009: fig. 4.3; Ekdale and Rowe 2011: fig. 3), *Zalambdalestes lechei* (Ekdale 2009: fig. 4.5; Ekdale and Rowe 2011: fig. 6), *Ukhaatherium nessovi* (Ekdale 2009: fig. 4.5); (ii) other early pan-euungulates *Hyopsodus lepidus* (Ravel and Orliac 2015), *Xenicohippus osborni* (Perissodactyla, Ravel and Orliac 2015), *Diacodexis ilicis* (Artiodactyla, Orliac et al. 2012); and (iii) South American ungulates including specimens of notoungulates and litopterns from the late Paleocene-early Eocene Beds of Itaboraí, Brazil (Billet and Muizon 2013; Billet et al. 2015). The South American ungulates are included because they have been recently proposed to be members of Euungulata, and more precisely Panperissodactyla (Buckley 2015; Welker et al. 2015).

Micro-CT Scanning and Digital Extractions

The petrosal AMNH-VP 118359 was scanned using the high-resolution micro-CT scanner in the Department of Biomedical Engineering, Stony Brook University, New York. The scans resulted in 1276 slices with a resolution of 5 μm. We extracted the digital endocast of the bony labyrinth and reconstructed the blood vessel canals and nerve pathways using the segmentation tools of AVIZO 8.0 (FEI Visualization Sciences Group) and calculated volumes by surface integration. Because of the presence of sediment and recrystallization in the bony labyrinth space, the segmentation process was carried out slice-by-slice manually with the limited range only option of the brush tool of AVIZO 8.0. We segmented the cochlea in a separate labelfield module to estimate its volume separately. The proximal limit of the cochlea was determined by the proximal extension of the primary and secondary bony laminae; it passes on a line joining the ventral border of the fenestra vestibuli to the dorsal edge of the fenestra cochleae. The blood vessel canals and nerve pathways were also segmented in separate labelfields. Additional images of the specimen, including stereoscopic views are available at MorphoBank.com (project #2290).

Measurements and Calculations

Linear measurements were taken using the 3D measurement tool of AVIZO 8.0 and the curve info option of ISE-Meshtool (Lebrun 2014). Measurements were made from the center of each canal following Spoor et al. (2007) and following the

protocol illustrated by Ekdale and Rowe (2011) and Ekdale (2013). We determined the number of cochlear turns according to the protocol described in Geisler and Luo (1996), also used in Ekdale and Rowe (2011) and Ekdale (2009, 2013). Angles were taken between the planes of all of the semicircular canals, when the planes were oriented perpendicular to the field of view, following Ekdale (2010). For each canal, the radius of curvature was calculated using the equation of Spoor and Zonneveld (1998) [(0.5 (l + w)/2), where l is the maximal length, measured from the point of the canal farthest away from the vestibule, and w is the maximal width of canal, measured perpendicular to the length line, at the widest expanse of the canal arc]. The length of the secondary bony lamina was measured as illustrated by Ekdale and Rowe (2011: fig.1) using 3D curves of ISE-Meshtool (Lebrun 2014) from the beginning of the laminar gap (located slightly medial to the medial border of the fenestra vestibuli) to the apex of the cochlea.

We calculated the range of hearing frequency limits at 60 dB using the power functions of Rosowski and Graybeal (1991) and Rosowski (1992) based on basilar membrane length (BM): Low-frequency Limit at 60 dB SPL (LF) = $13BM^{-1.2}$; High-frequency Limit at 60 dB SPL (HF) = $391BM^{-0.85}$, and footplate area (FP): Low-frequency Limit (kHz) = $0.40FP^{-1.1}$; High-frequency Limit (kHz) = $34FP^{-0.40}$. Footplate area was estimated from the area of the fenestra vestibuli. We also used the power function of West (1985) combining both cochlear coiling (N) and basilar membrane length (BM) log (LF) = 1.76–1.66 log (BMxN); log (HF) = 2.42–0.994 log (BM/N). These power functions were used by Meng and Fox (1995) to estimate the frequency limits in fossil therians from the Bug Creek Anthills. Manoussaki et al. (2008) demonstrated that the radii ratio of the cochlea (quotient of the radius of the basal turn (Rbase) and the radius of the apical turn (Rapex) of the cochlea) was linearly correlated with the log of low-frequency hearing abilities limit for a sample of mammal species. We use the equation of Manoussaki et al. (2008) to predict low-frequency hearing limit: LF = 1.507 exp.[−0.578(p-1)], with p = radii ratio = Rbase/Rapex. The relationship of radii ratio and LF proposed by Manoussaki et al. (2008) has higher significance level and correlation coefficient than the relationship proposed by West (1985). However, the construction procedure of Manoussaki et al. (2008) to determine Rbase and Rapex is not straightforward and might differ depending on the author (Danilo 2012; Danilo et al. 2015; Ekdale and Racicot 2015). We measured the radii of curvature (Rbase and Rapex) following the procedure of Manoussaki et al. (2008) with five equidistant points. We placed those points along the arcs of circles of the first and last quarter of turn of the line passing in the middle of the cochlear canal.

Description

Cast of the Bony Labyrinth

The bony labyrinth of *Protungulatum* largely fills the petrosal volume (Fig. 1). The cochlea occupies most of the volume of the pars cochlearis and the semicircular canals are spread widely through the mastoid region of the pars canalicularis. The dorsal margin of the wide subarcuate fossa is bordered by the anterior semicircular canal (Fig. 1a-c); the mastoid region is excavated by the very deep subarcuate fossa that extends well posterior to the lateral and posterior semicircular canals (Fig. 1c). Measurements of the 3D reconstruction of the labyrinth endocasts of *Protungulatum* and a comparison sample of ungulates and early diverging eutherians are provided in Table 1.

Cochlear Canal

The cochlea contributes 60.8 % of the total volume of the bony labyrinth of *Protungulatum* (Table 1). The coiling of the cochlear canal completes 1.54 turns (rotation of 553°). While not fully planispiral, the cochlear canal lies nearly in a single plane with an aspect ratio of 0.51 (Table 1). The second turn tightly contacts the basal turn (Fig. 2). The diameter of the cochlear canal is roughly constant and decreases only slightly towards the apex. The portion of the cochlea immediately anterior to the cochlear aqueduct (canaliculus cochlearis), has a slightly larger diameter (see discussion in "Reconstruction of Blood Vessels" section below). The primary bony lamina (lamina spiralis ossea primaria, projecting from the modiolus and marking the division between the scala tympani and the scala vestibuli of the cochlear canal; Meng and Fox 1995) runs on the internal wall of the cochlear canal and stops abruptly shortly before the helicotrema (see online supplementary material Fig. O1). The secondary bony lamina (lamina spiralis ossea secundaria, projecting from the outer wall of the cochlear canal) leaves a deep groove on the cochlear cast that vanishes shortly before the end of the basal turn at around 340°. The extension of the secondary bony lamina covers around 61 % of the cochlear canal length. The course of the secondary bony lamina on the external wall along the cochlear canal shows that the scala tympani is as high as the scala vestibuli in the proximal part of the cochlea, and diminishes in height at the end of the first turn. The laminar gap between the primary and secondary bony laminae is narrowest at the base of the cochlea and the width of the basilar membrane continuously increases towards the apex (see online supplementary material Fig. O1).

We make a distinction between the internal fenestra cochleae, which in living mammals is closed by the secondary tympanic membrane, and the more external aperture of the tympanic opening of the recess of the cochlear fossula (fossula fenestra

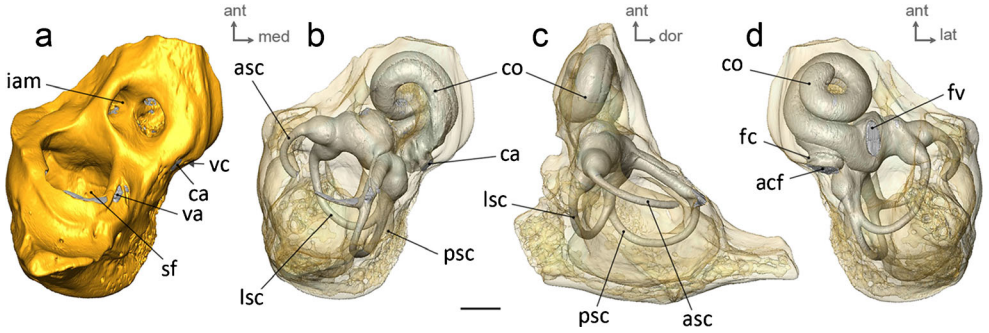

Fig. 1 In-situ 3D reconstruction from CT data of the bony labyrinth of a left petrosal of *Protungulatum* sp. (AMNH-VP 118359). Specimen illustrated in (**a**-**b**) dorsomedial, (**c**) lateral, and (**d**) ventrolateral views. *Scale bar* =1 mm. Abbreviations: acf, external aperture of cochlear fossula; asc, anterior semicircular canal; ca, cochlear aqueduct; co, cochlear canal; fc, fenestra cochleae; fv, fenestra vestibuli; iam, internal acoustic meatus; lsc, lateral semicircular canal; psc, posterior semicircular canal; sf, subarcuate fossa; va, vestibular aqueduct; vc, vein of the cochlear aqueduct

cochleae, Bast and Anson 1952; aperture of the cochlear fossula, MacPhee 1981; "outpocketing for perilymphatic sac" according to Ekdale 2009, 2013) (see online supplementary material Fig. O2). The cochlear fossula is immediately external to the fenestra cochleae and houses the perilymphatic sac (Bast and Anson 1952; Meng and Fox 1995; Wible et al. 2009:38; Ekdale 2009, 2013). The external aperture of the cochlear fossula of *Protungulatum* is small, elliptical, and located roughly about as far anteriorly as the posterior edge of the smaller fenestra vestibuli (Figs. 1d, 2e). The fenestra cochleae is clearly larger than the external aperture of the cochlear fossula (Figs. 1d and 2e-f, see also O'Leary 2010: fig. 3, cochlear fossula visible but unlabeled). The dorsal edge of the fossula bears a horseshoe shaped keel, extending anteriorly on the dorsal surface of the cochlear canal, and connecting medially to the root of the cochlear aqueduct (Figs. 2e and 3i). The cochlear aqueduct (housing the perilymphatic duct in life) is short and emerges at the dorsomedial edge of the fenestra cochleae and projects posteromedially (Fig. 2d-e). The fenestra vestibuli is oblong in shape, located at the level of the external aperture of the cochlear fossula, well below the level of the lateral semicircular canal (Fig. 2e). The stapedial ratio (calculated as the greatest length of the fenestra vestibuli divided by the greatest width perpendicular to the length) equals 2.1 (Table 1).

Table 1 Measurements of 3D reconstructions from CT data of bony labyrinth endocasts of *Protungulatum* sp. (AMNH-VP 118359), of the early euungulates *Hyopsodus lepidus* (AMNH143783, measurements partly from Ravel and Orliac 2015) and *Diacodexis ilicis* (AMNH VP 16141, measurements partly from Orliac et al. 2012), and of the Cretaceous eutherians *Kulbeckia kulbecke* and zhelestids (from Ekdale 2009, 2013)

	Protungulatum sp.	*H. lepidus*	*D. ilicis*	*K. kulbecke*	zhelestid
Stapedial ratio	2.1	1.44	1.78	2.00	1.6
Coclear aspect ratio	0.51	0.77	0.64	0.44	0.46
Cochlear coil	553°	792°	736°	446°	545°
Cochlear canal length	7.1	10.1	7.35	4.93	4.93
Labyrinth volume	5.1	11.5	11.77	5.37	6.28
Cochlea volume	3.1	7.19	6.53	2.59	4.15
Cochlea vol/vol tot	60.8 %	62.5 %	55.5 %	48.2 %	66.0 %
2° lamina coil*	340° - 61 %	135° - 17 %	180° - 24 %	209° - 47 %	198° - 36 %
Angle ASC/LSC	74°	91.5°	73°	79.9	88.8
Angle LSC/PSC	98°	91°	81°	89.6	93.1
Angle ASC/PSC	81°	84°	95°	79.9	96.8
ASC H/W	2.46/2.27	3.12/2.81	3.49/3.36		
ASC R/L	1.18/5.97	1.48/7.2	1.71/8.69	1.19/5.70	1.17/5.80
PSC H/W	2.16/1.94	2.43/2.36	2.39/3.09		
PSC R/L	1.02/5.79	1.19/7.1	1.37/7.68	0.96/4.55	0.86/4.62
LSC H/W	1.95/1.82	2.34/2.14	2.17/2.79		
LSC R/L	0.94/4.23	1.12/5.34	1.24/5.05	0.92/3.94	0.79/3.49

*2° lamina extension expressed as a percentage of cochlear length. Abbreviations: ASC, anterior semicircular canal; LSC, lateral semicircular canal; PSC, posterior semicircular canal; following a semicircular canal name: H, height; L, length (comprising the common crus for ASC and PSC); R, radius; W, width. Measurements are given in mm (linear measurements) and mm^3 (volumes)

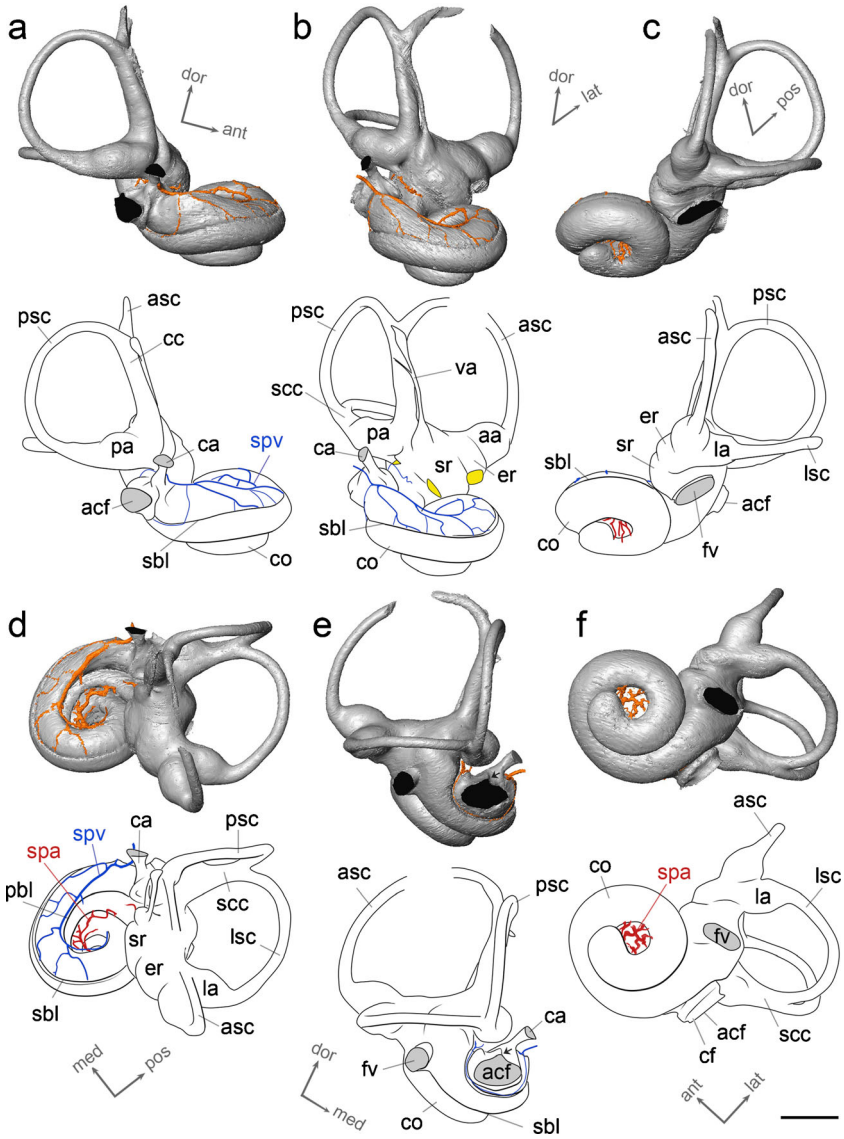

Fig. 2 Virtual 3D reconstruction and outline drawing of the left bony labyrinth cast of *Protungulatum* sp. (AMNH-VP 118359) in (**a**) posterior, (**b**) medial, (**c**) anterior, (**d**) dorsal, (**e**) lateral, and (**f**) ventral views. *Scale bar* =1 mm. Abbreviations: aa, anterior ampulla; acf, external aperture of cochlear fossula; asc, anterior semicircular canal; ca, cochlear aqueduct; cc, common crus; cf., cochlear fossula; co, cochlear canal; er, elliptical recess; fv, fenestra vestibuli; la, lateral ampulla; lsc, lateral semicircular canal; pa, posterior ampulla; pbl, primary bony lamina imprint; psc, posterior semicircular canal; scc, secondary common crus; sbl, secondary bony lamina (imprint); spa, spiral modiolar artery; spv, spiral modiolar vein; sr, spherical recess; va, vestibular aqueduct. Nerve pathway are colored in *yellow*, openings toward the external surface of the petrosal are colored in *black* (3D model) and *light grey* (drawings); blood vessels reconstructed in *orange* on the 3D models; veins in *blue* and arteries in *red* on the drawings; *black arrow* in (**e**) indicates dorsal swelling of the external aperture of cochlear fossula in relation with the horseshoe shaped keel

Vestibule and Semicircular Canals

In *Protungulatum*, the distinction between the spherical and elliptical recesses is clear and the swelling of the small elliptical recess is visible in dorsal and anterior views of the labyrinth (Fig. 2b-d). The spherical recess is visible as a bulge extending from the elliptical recess to the base of the vestibular aqueduct, laterally in anterior view, and between the fenestra cochleae and the fenestra vestibuli in posterior view. The vestibular aqueduct (housing the endolymphatic duct in life) originates at the basis of the common crus, slightly anterior to it, and has a bulged base, extending inferior to the level of the common crus (Fig. 2b). The vestibular aqueduct is shorter than the height of the common crus, its dorsal-most part is divided into two small canals (Fig. 2b).

The anterior semicircular canal (ASC) of *Protungulatum* shows the greatest extent dorsally and has the greatest radius of any of the three semicircular canals (Table 1). Its dorsal-most part is slightly bent anteriorly (Fig. 2c). The posterior semicircular canal (PSC) is smaller than the ASC; it is also slightly bent laterally relative to the horizontal plane. The posterior limb of the lateral semicircular canal (LSC) fuses with the PSC in a short secondary common crus (Fig. 2a,d,f) in which the courses of both canals can be distinguished. The ASC is straight along its course and lies in a single plane (Fig. 2). The LSC and PSC are slightly sigmoidal (Fig. 2e): the LSC is slightly deflected dorsally along its midsection, while the PSC is slightly laterally deflected along its midsection. In contrast to the PSC, which has a regular profile, the ASC and LSC follow more elliptical arcs pointing towards the PSC (Fig. 2d-e). The angle between the ASC and LSC is the smallest of all; and the angle between the PSC and LSC is the widest (Table 1). The outer bony casing that would have held the anterior ampulla in life is slightly more inflated than the

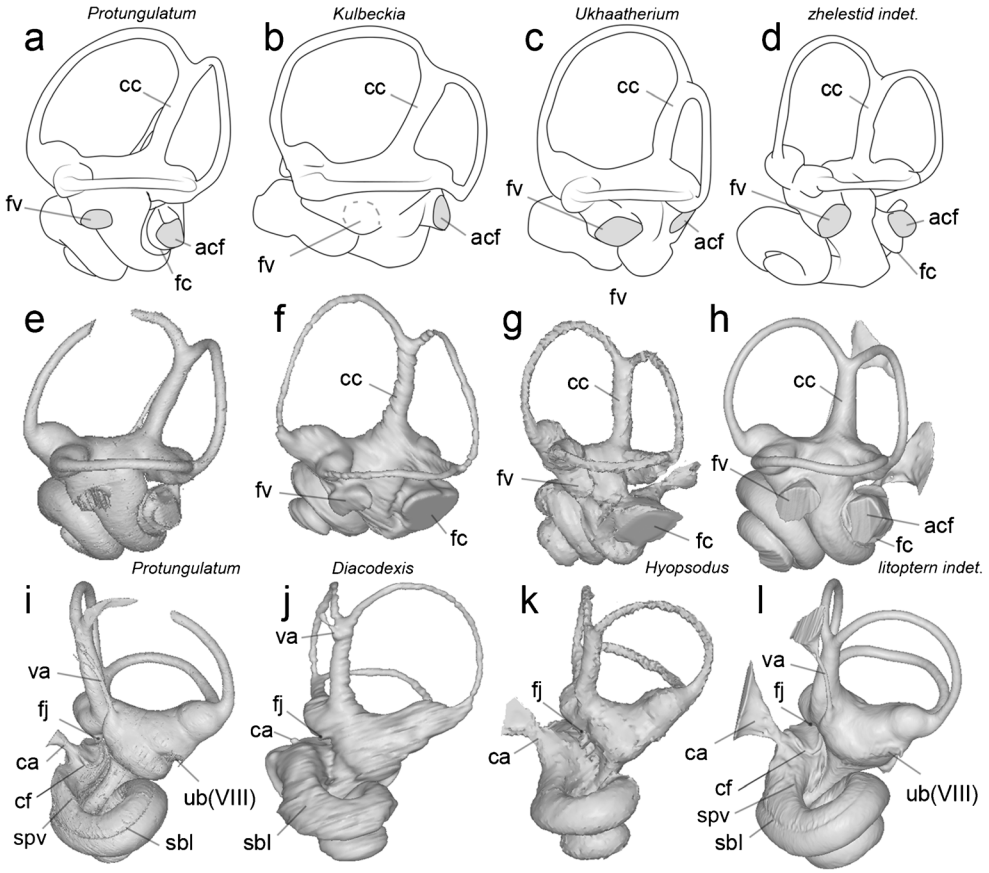

Fig. 3 Comparison of the bony labyrinth morphology of *Protungulatum* sp. to Late Cretaceous non-placental eutherian and pan-euungulate mammals. Taxa illustrated are (**a**, **e**, **i**) *Protungulatum* sp. (AMNH-VP 118359), (**b**) *Kulbeckia kulbecke* (after Ekdale 2009: fig. 4.5D), (**c**) *Ukhaatherium nessovi* (after Ekdale 2009: fig. 4.5B), (**d**) zhelestid indet. (after Ekdale 2009: fig. 4.3C), (**f**, **j**) *Diacodexis ilicis*, (**g**, **k**) *Hyopsodus lepidus*, (**h**, **l**, mirror view) litoptern indet., (UFRJ-DG 119-M, Billet et al. 2015). (**a**-**h**) lateral views, (**i**-**j**) mediodorsal view. Not to scale. Abbreviations: acf, external aperture of cochlear fossula; ca, cochlear aqueduct; cc, common crus; cf., cochlear fossula; co, cochlear canal; fc, fenestra cochleae; fj, foramen jugulare; fs, foramen singulare (ampular branch of vestibulocochlear nerve); fv, fenestra vestibuli; sbl, secondary bony lamina imprint; spv, spiral modiolar vein; ub (VIII), connection with utricular branch of vestibulocochlear nerve; va, vestibular aqueduct

posterior and lateral ampullae (Fig. 2). The posterior ampulla attaches to the vestibule at the level of the LSC horizontal plane, whereas the anterior ampulla is located slightly above this plane (Fig. 2e). The long axis of the common crus points dorsally in the posterior direction; the distance between the base of the common crus and the anterior ampulla is long and the common crus forms a widely open angle with the dorsal border of the vestibule at the level of the ASC.

Reconstruction of Facial (VII) and Vestibulocochlear (VIII) Nerve Pathways

Two cranial nerves enter the internal acoustic meatus of mammals in life: (i) the facial nerve (VII) passes through the foramen acusticum superius, and (ii) the vestibulocochlear nerve (VIII), which divides into two main branches and passes both through the foramen acusticum superius and inferius (Wible 2003:160–161). The exceptional preservation of AMNH-VP 118359 permitted us to reconstruct the pathways of both nerves in fine detail based on grooves and canals in the bone (Fig. 4). In life, the vestibular part of the vestibulocochlear nerve is distributed to the ampullae of the semicircular ducts (ampular branches) and to the maculae of the utricle and saccule (utricular and saccular branches) (Barone and Bortolami 2004). The endocast of the bony labyrinth of *Protungulatum* clearly shows the pathways corresponding to these connections of the vestibular part of the vestibulocochlear nerve to the spherical and elliptical recesses (via the area cribrosa media and area cribrosa superior, respectively), as well as a connection to the posterior ampulla of the semicircular canal (Figs. 2b, 4c-j and 5a). The connection to the posterior ampulla of the semicircular canal corresponds to the foramen singulare located in the foramen acusticum inferius (Wible 2010). The foramen acusticum inferius also houses the cribriform plate of the modiolus (Fig. 4b), the conical shaped central bony axis of the cochlea (Fig. 5a-b). The cribriform plate

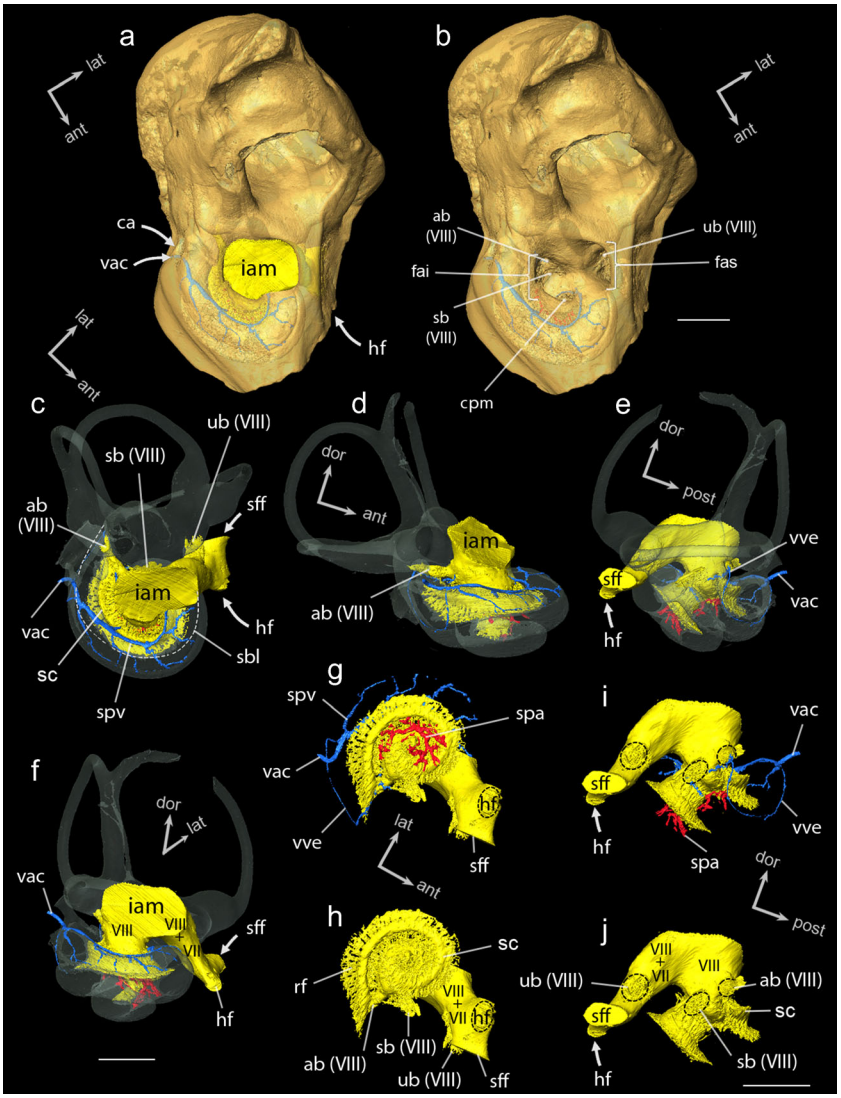

Fig. 4 Virtual 3D reconstruction of the innervation and vasculature of the left bony labyrinth of *Protungulatum* sp. (AMNH-VP 118359). (**a**-**b**) general view of the foramina of the petrosal related to innervation and vasculature of the bony labyrinth viewed though a translucent rendering of the petrosal; (**c**-**f**) innervation and vasculature of the bony labyrinth viewed though a translucent rendering of the bony labyrinth (*light gray*) in (**c**) dorsal, (**b**) posteromedial, (**c**) lateral, and (**f**) medial views; (**g**-**j**) innervation and vasculature of the cochlea in (**g**-**h**) ventromedial, and (**i**-**j**) lateral views. Reconstruction of the vestibulocochlear nerve in *yellow*, veins in *blue*, and arteries in *red*, secondary bony lamina in *white dotted line*. *Scale bars* =1 mm. Abbreviations: ab (VIII), ampular branch of vestibulocochlear nerve (foramen jugulare); cpm, cribriform plate of the modiolus; fai, foramen acusticum inferius; fas, foramen acusticum superius; hf, hiatus Fallopii; rf, radiating fibers; sb (VIII), saccular branch of vestibulocochlear nerve (area cribrosa media); sbl, secondary bony lamina; sc, spiral ganglion canal; sff, secondary facial foramen; spa, spiral modiolar artery; spv, spiral modiolar vein; ub (VIII), utricular branch of vestibulocochlear nerve (area cribrosa superior); vac, vena aquaeductus cochleae canal; vve, veina vestibularis; VII, cranial nerve VII (facial nerve); VIII, cranial nerve VIII (vestibulocochlear nerve)

of the modiolus (tractus spiralis foraminosus) is composed of several foramina for nerves connecting the cochlear part of cranial nerve VIII and the spiral ganglion (Meng and Fox 1995). The modiolus of *Protungulatum* is thick and pierced by abundant and rather large foramina (Fig. 5b). The spiral ganglion (composed of the cell bodies of the most peripheral nerve cells of the acoustic system, which receive information from the sensory cells of the organ of Corti) is housed in the spiral canal (canalis spiralis modioli) located in the modiolus. In *Protungulatum*, the spiral canal is wide and its diameter extends dorsally past the level of the primary bony lamina, on the internal wall of the cochlear canal Fig. 5a. The spiral canal is easy to visualize on the 3D reconstruction of the cochlear nerve pathway, in lateral and ventral views (Fig. 4h). The pathway of the cochlear fibers from the organ of Corti to the spiral ganglion can be reconstructed from the space between the two layers of the primary bony lamina: close to the laminar gap (location of the basilar membrane holding the organ of Corti in life) the nerve fibers distribute in a loose network; they gather through small tubuli before

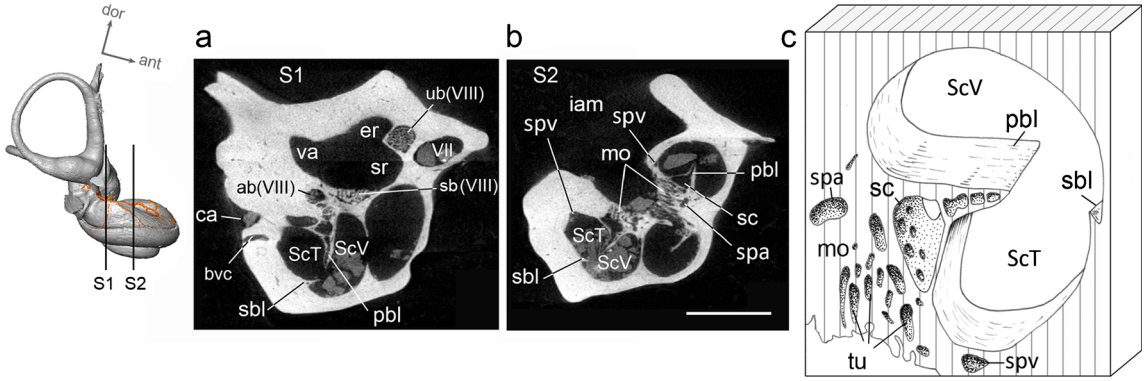

Fig. 5 Computed-tomography slices through the isolated petrosal of *Protungulatum* sp. (AMNH-VP 118359) and "block picture" (Fleischer 1973, 1976) of the basal turn structure. S1 and S2 correspond to the location of slices (**a**-**b**) on the bony labyrinth; (**c**) block picture of the cochlea. *Scale bar*: 1 mm. Abbreviations: ab(VIII), ampular branch of vestibulocochlear nerve; ca, cochlear aqueduct; er, elliptical recess; iam; internal acoustic meatus; mo, modiolus; pbl, primary bony lamina; sbl, secondary bony lamina; spv, spiral modiolar vein; sr, spherical recess; ScT, scala tympani; ScV, scala vestibuli; sc, spiral ganglion canal; spa, spiral modiolar artery; tu, tubuli of the modiolus; ub(VIII), utricular branch of vestibulocochlear nerve; va, vestibular aqueduct; vac, vena aquaeductus cochleae; VII, facial nerve

they enter the spiral canal, perpendicularly (Fig. 4h). Fig. 4 illustrates the distribution of what would have been the pathway of cochlear nerve fibers though the cribriform plate of the modiolus and through the primary bony lamina where they radiate in a fan-shaped network of tubuli. The morphology of the modiolus and cochlear canal of *Protungulatum* is summarized in a schematic cochlear turn diagram (Fig. 5c), or "block picture" inspired by that of Fleischer (1973) and corresponding to the morphology of the basal turn shortly after the fenestra cochleae (Fleischer 1976:figs.1-2). Compared to block pictures of Artiodactyla (ruminants [*Capreolus* and *Giraffa*] and tylopod [*Camelus*]), and Perissodactyla (*Tapirus* and *Equus*) (Fleischer 1973: figs.110-114), the spiral canal of *Protungulatum* is wider and extends more onto the scala tympani.

Reconstruction of Blood Vessels

The vasculature of the cochlea plays an important role in its function. Cochlear blood supply derives from the labyrinthine artery, a branch of the anterior inferior cerebellar artery (Gray 1918) and distributes inside the inner ear via the spiral modiolar artery in mammals (Axelsson and Ryan 1988). In *Protungulatum*, the main blood vessel canal etched into the bone of the modiolus most likely corresponds to the spiral modiolar artery (Figs. 2d,f, 4e-g,i and 5), which ascends in a spiral pattern around the modiolus (Fig. 5b) from the base to the apex. The canal for the spiral modiolar artery and its radiating arterioles can be reconstructed to the apex of the cochlea (Figs. 2 and 4). The modiolar artery enters the petrosal through a small foramen located in the foramen acusticum inferius on the edge of the proximal part of the cribriform plate of the modiolus. Another important blood vessel impression visible on the dorsal surface of the basal turn of the cochlea (Figs. 2, 4 and 5) may correspond to the vena aquaeductus cochleae. It leads to a small foramen lying next to the cochlear aqueduct foramen on the petrosal (Fig. 1a and 4a); on the basal turn of the cochlear canal, it is accompanied by radiating secondary venule bony imprints originating at the level of the secondary spiral bony lamina (Figs. 2 and 4). The course of the channels continues posteriorly and ventrally below and around the cochlear fossula, lining the proximal most portion of the secondary spiral bony lamina (Figs. 2e and 4), and reaching the vestibule medially. This pattern of vessels is interpreted here as the vena ditto cochleae (Frick et al. 1992; Feneis 1993; or vena canaliculi cochleae, Schaller et al. 1992), spiral modiolar vein (veina spiralis modioli, Schaller et al. 1992) and confluent venules, and the veina vestibularis. In life, the spiral modiolar vein empties into the vein of the cochlear aqueduct and receives collecting venules from the scala tympani, the spiral lamina, and the capillary area in the modiolus (Axelsson and Ryan 1988). This system is the principal drainage of the inner ear and drains the blood from the basal cochlear turn and from the vestibule. In *Protungulatum*, the canal of the vein of the cochlear aqueduct is distinct from the cochlear aqueduct itself (Figs. 2b,e and 4).

Comparisons

Comparison with Previously Described Inner Ears of Eutherian Mammals from Bug Creek Anthills and Contribution of CT Scan Data

The morphology and dimensions of the specimen described in MacIntyre (1972: figs. 4-5) are generally compatible with the *Protungulatum* specimen described here. However, differences in the preservation of the two specimens indicate that the specimen illustrated by MacIntyre (1972: fig. 4) is not the specimen described here (see online supplementary material

Fig. O3). Randomly fractured fossil petrosals of eutherian mammals from Bug Creek, Montana, permitted MacIntyre "a reasonable reconstruction of the labyrinth from fossils, with some limits" (MacIntyre 1972:284). The exact number of specimens on which this reconstruction is based is not mentioned. Further observations of broken petrosals from Bug Creek were performed by Meng and Fox (1995) who differentiated marsupials and placentals, based on direct observation of the internal anatomy with scanning electron microscopy and radiographs. The specimens figured by Meng and Fox (1995: figs. 1A, 2, 3A) are close morphologically to AMNH-VP 118359 (see online supplementary material Fig. O4) and measurements are similar (Table 1 vs Meng and Fox 1995: table 1).

Meng and Fox (1995:58) did not assign the placental petrosals from Bug Creek Anthills to either the 'ferungulate' or 'unguiculate' types of MacIntyre (1972) and regarded them as placental petrosals collectively. Three dimensional reconstruction of the inner ear of AMNH-VP 118359 referred to *Protungulatum* shows a few differences with the reconstruction of the placental inner ear provided by Meng and Fox (1995: fig. 3). Those differences concern the shape of the basal turn, the orientation of the cochlear axis, the orientation of the common crus, and the length of the secondary common crus. These differences might be due either to the fact that these specimens represent two different taxa, or to interpretation bias related to reconstruction based on broken specimens and radiographs in Meng and Fox (1995: fig. 3). Meng and Fox (1995) also described in detail the innervation of the cochlea of eutherians from Bug Creek. Our CT scan investigation and three dimensional reconstruction of the finest structure of the bony labyrinth of AMNH-VP 118359 lead us to similar observations (weak cochlear coiling, long secondary osseous spiral lamina, radial pattern of the cochlear nerve) and allow us to contribute additional information. New information from our work includes: 1) direct visualization of the inner ear, including the radial network of the cochlear nerve dendrites and of the blood supply of the cochlea; 2) corroboration of the location of the connection of cranial nerve VIII to the saccule (area vestibularis media, Meng and Fox 1995) in the lateral wall of the foramen acusticum inferius [sb(VIII) on Fig. 3]; and 3) the first observation of a horseshoe shape structure of the "perilymphatic recess."

Comparisons with Late Cretaceous Eutherians and Early Pan-Euungulates

Cochlear Canal The coiling of the spiral canal of the cochlea of *Protungulatum* fits in the range of variation described for zhelestids but exceeds that of other described Cretaceous eutherians *Kulbeckia*, *Uklaatherium*, and *Zalambdalestes* (Ekdale 2009). It is markedly weaker than that of described Paleogene pan-euungulates *Hyopsodus lepidus* (rotation of 792°; Ravel and Orliac 2015), *Diacodexis ilicis* (rotation of 736°; Orliac et al. 2012), and extinct South American notoungulate *Notostylops murinus* (rotation of 810°, protocol of West 1985; Macrini et al. 2010), and Litopterna from Itaboraí (minimal rotation of 810°; Billet et al. 2015). The extent of the secondary bony lamina of *Protungulatum* is comparable to that of Late Cretaceous non-placental eutherians such as *Kulbeckia* and zhelestids described by Ekdale (2009; 1/4 to 3/4 of the first turn), and greater than that of *Zalambdalestes lechei* (Ekdale 2009; 1/4 of the first turn). It is largely superior to the extent observed in the pan-euungulates *H. lepidus* (17 %) and *D. ilicis* (24 %). The extent of the secondary bony lamina in *Protungulatum* is also greater than that of litoptern specimens from Itaboraí, Brazil (cf. *Miguelsoria parayirunhor*, Billet et al. 2015; 1/4 to 3/4 of the first turn). In *Protungulatum*, the laminar gap between the primary and secondary bony laminae is narrowest at the base of the cochlea and it continuously increases towards the apex (see online supplementary material Fig. O1), which is also the case for Cretaceous eutherians (Ekdale and Rowe 2011: fig. 5).

The cochlear fossula, observed in *Protungulatum*, is not present in *Kulbeckia* and zhelestids (Ekdale 2009; Ekdale and Rowe 2011: figs. 3B, 6C), but is observed in the early notoungulate described by Billet and Muizon (2013) and in litopterns (Billet et al. 2015: fig. 7). The cochlear fossula is not observed on the bony labyrinth of the pan-euungulates *Diacodexis ilicis* (Orliac et al. 2012; Orliac and O'Leary 2014: fig. 2) and *Hyopsodus lepidus* (Ravel and Orliac 2015). Unfortunately, the poor preservation of the inner ear of *Xenycohippus osborni* does not permit clear observation. However, we do note that the early equoid *Palaeotherium muehlbergi muehlbergi* (UM 1756, Gypse de Paris, MP19) has no cochlear fossula (Danilo 2012: fig. 4.50). The outpocketing lateral to the base of the bony channel of the cochlear aqueduct observed in *Protungulatum* is also observed in *Kulbeckia*, *Zalambdaleste lechei*, and zhelestids (Ekdale and Rowe 2011: figs. 3B, 6C) but it forms a larger pocket that is not horseshoe shaped (see online supplementary material Fig. O5). This outpocketing lateral to the base of the cochlear aqueduct is also present in the litoptern specimens studied in Billet et al. (2015: fig. 9), as illustrated in Fig. 3l, where it has a horseshoe shape identical to that observed in *Protungulatum*. It is, however, not clear in the pan-euungulate *H. lepidus* or in the artiodactyl *D. ilicis* (Fig. 3i-l), but this could be due to limited quality of the reconstruction. Early artiodactyls such as *Homacodon* or *Helohyus*, however, lack a horseshoe shaped keel (Orliac and O'Leary 2011). Again, the poor preservation of the inner ear of *Xenycohippus osborni* does not permit clear observation of this keel. The early equoid *Palaeotherium* has no keel (Orliac pers. obs.) As this structure might represent an anterior extension of the cochlear fossula, its absence might be correlated with the

absence of wide cochlear fossula in artiodactyls and perissodactyls. The orientation of the cochlear aqueduct of *Protungulatum* is similar to the orientation observed in the Late Cretaceous zhelestid figured by Ekdale (2009: fig. 4.3). This orientation is more anteriorly-directed than in *Kulbeckia* and *Zalambdalestes lechei* (Ekdale and Rowe 2011: fig. 6). It is also more anterior than in *H. lepidus* (compare Ravel and Orliac 2015: fig. 2c, e and *D. ilicis* (Orliac et al. 2012). The angle formed by the planes of the first turn of the cochlea and the LSC is more open in *Protungulatum* than in Late Cretaceous eutherian mammals (as figured by Ekdale 2009: fig. 4.3, 4.5; 2013: fig. 6) and is closer to the configuration observed in the pan-euungulate *H. lepidus*, in the artiodactyl *D. ilicis*, in Litopterna (Billet et al. 2015) (Fig. 3a-h), and in early diverging notoungulates (Macrini et al. 2010; Billet and Muizon 2013).

Vestibule The gross morphology of the vestibular apparatus is in general accordance among all of the Late Cretaceous eutherians examined by Ekdale and Rowe (2011), *Protungulatum*, and the early pan-euungulates *H. lepidus*, *D. ilicis*, and *X. osborni*. A secondary common crus is present in all specimens. As in the Late Cretaceous eutherians *Kulbeckia*, *Zalambdalestes*, and zhelestids (Ekdale and Rowe 2011: figs. 3, 6), the root of the bony channel for the vestibular aqueduct is located anteromedial to the common crus. The bony vestibule of *Protungulatum* is morphologically similar to that of *Diacodexis*, which also shows a clear distinction between spherical and elliptical recesses, both of which are bulged (Orliac et al. 2012). In *Protungulatum* and *Diacodexis*, the expansion of the spherical recess below the common crus is more pronounced than in *H. lepidus* and *X. osborni* (Ravel and Orliac 2015). Compared with *D. ilicis* and *H. lepidus*, and as in Late Cretaceous eutherians, *Protungulatum* shows a more ventral position of the fenestra vestibuli relative to the ventral edge of the lateral ampulla. Compared to the litopterns figured by Billet et al. (2015: fig. 7), *Protungulatum* shows a more pronounced expansion of the spherical recess below the common crus and a larger and more salient elliptical recess. As in *Protungulatum* and Late Cretaceous eutherians, *H. lepidus* and litopterns from Itaboraí present an anteromedial location of the bony channel for the vestibular aqueduct relative to the base of the common crus. *Protungulatum* and litopterns from Itaboraí further share a bulged base of the vestibular aqueduct canal (Billet et al. 2015: fig. 7). This character is not observed in notoungulate inner ears published by Macrini et al. (2013), but is present in a notoungulate specimen from Itaboraí (Billet and Muizon 2013: fig. 5D). In *D. ilicis*, and *Palaeotherium muehlbergi*, however, the bony channel for the vestibular aqueduct originates from the base of the common crus.

Semicircular Canals In AMNH-VP 118359, as in *Kulbeckia*, the widest angle occurs between the LSC and the PSC, whereas in *Ukhaatherium* and in zhelestids, the ASC/PSC angle is the widest (Table 1). This condition is also the case in *Diacodexis*. In *Protungulatum*, the long axis of the common crus points dorsally and in a posterior direction, and the distance between the basis of the common crus and the anterior ampulla is long compared to the same distance in *D. ilicis* and *H. lepidus* (Fig. 3e vs. 3f-g). A comparable orientation of the common crus is observed in the Late Cretaceous eutherians *Ukhaatherium* (Ekdale 2009: fig. 4.5) and *Kulbeckia* (Ekdale 2013: fig. 6) (Fig. 3b-c). This peculiar orientation is, to our knowledge, not observed in other published accounts of pan-euungulate inner ears. AMNH-VP 118359 is also morphologically similar to Late Cretaceous eutherians in the long distance between the base of the common crus and the anterior ampulla. This distance is shorter in pan-euungulates as well as in litopterns (Billet et al. 2015: fig. 7C) and notoungulates (Billet and Muizon 2013; Macrini et al. 2013).

Nerve and Blood Vessel Pathways Very few data are available yet about the reconstructed morphology of inner ear nerve pathways and pattern of blood vessels in fossil eutherians. A challenging obstacle has been that these fragile and subtle structures may be particularly affected by poor preservation or insufficient resolution of CT scan data. Slices through the cochlea of *Kulbekia* (Ekdale 2009: fig. 5.7) showed a structure generally close to what we observe in *Protungulatum*: a thick modiolus, wide spiral canal, and large canal for the spiral modiolar artery. However, there is no trace of the spiral modiolar vein canal on the available slices for *Kulbekia*. Slices through the zhelestid petrosal (Ekdale and Rowe 2011: fig. 4) show a similar structure: the spiral canal is wide, but the modiolus seems to be thinner.

Slices through the cochlear canal of a notoungulate petrosal from Itaboraí illustrated by Billet and Muizon (2013: fig. 6) and a litoptern from the same locality (Billet et al. 2015: fig. 9) seemed to show a relatively thin modiolus compared to *Protungulatum*; however this difference could be due to a higher coiling of the cochlea, or to differences in slice location (more distal in Billet and Muizon 2013 and Billet et al. 2015). The spiral canal seems to be wider in *Protungulatum* than in the litoptern and notoungulate from Itaboraí. Slices through the cochlea of the litoptern clearly show the spiral vein canal, whereas this canal is absent on the notoungulate slices. These species further differ in the density of tubuli at the level of the scala tympani, the litoptern being similar to *Protungulatum*, with a low number of tubuli. Comparisons with *Diacodexis* are difficult because of taphonomic recrystallization inside the bony labyrinth of the latter in the specimen examined here. The fine structures of the modiolus of *Hyopsodus* cannot be observed for the same reason, however, the modiolus appears to be rather thick, as in *Protungulatum*.

Blood vessels are rarely reconstructed in fossil bony labyrinths. Billet et al. (2015: figs. 7, 8) described the course of the vena aquaeductus cochleae on the proximal part of the basal turn of the cochlea in fossil litoptern UFRJ-DG 1035-M from Itaboraí. The morphology of the latter is very close to what is observed in *Protungulatum* (Fig. O6) and the small canal parallel to the cochlear aqueduct illustrated on the specimen UFRJ-DG 347-M (Billet et al. 2015: fig. 7C-D) most probably represents the pathway of the exit of the vena aquaeductus cochleae. A small canal parallel to the cochlear aqueduct also exists in some unpublished notoungulate petrosals from Itaboraí (G. Billet pers. comm.). Unfortunately, the resolution and contrast quality of the CT-scan data of *Diacodexis ilicis* and *Hyopsodus lepidus* do not permit reconstruction of the cochlear blood vessels. But there is no trace of the vena aquaeductus cochleae on the dorsal part of the basal turn of the cochlear canal of these two taxa, suggesting a somewhat different course of this structure: maybe internal to the cochlear canal. The same is true for Cretaceous eutherians (Ekdale and Rowe 2011: fig. 6).

Interpretation of the Auditory Capability of *Protungulatum*

The cochlear canal of AMNH-VP 118359, completing 1.5 turns, is short compared to most extant placental mammals (Ekdale 2013). However, in living placentals, some Lipotyphla (e.g., *Erinaceus*, *Sorex*), Tenrecomorpha (*Hemicentetes*), and Sirenia (*Trichechus*) have a cochlea with a coiling equal or below one and a half turns (Gray 1908; Lewis et al. 1985; Ekdale 2013). Mammals with a short basilar membrane are most sensitive to high-frequency sounds (West 1985; Rosowski and Graybeal 1991). We calculated the range of hearing frequency limits at 60 dB for AMNH-VP 118359 using the power functions provided by Rosowski and Graybeal (1991) and Rosowski (1992) based on basilar membrane length and footplate area (here estimated from the area of fenestra vestibuli). Using basilar membrane length, an upper limit of 73.91 KHz and a lower limit of 1.21 KHz are obtained. Using footplate area, an upper limit of 57.66 1 KHz and a lower limit of 1.71 KHz are obtained. We also used the equation of West (1985) combining both cochlear coiling and basilar membrane length. An estimate for the upper limit of 57.21 KHz and an estimate for the lower limit of 1.091 KHz are obtained. We also calculated the low frequency limit using the equation of Manoussaki et al. (2008). The radii ratio (Rbase/Rapex) equals 1.7, which corresponds to a calculated low frequency limit of 1.005 KHz. The estimated low frequency limits are above 1 KHz, which is above the limits in living terrestrial mammals (West 1985). Meng and Fox (1995) calculated high and low frequency limit estimates for Bug Creek Anthills placentals and obtained a range between 87.70 and 55.89 KHz for high frequency limit estimates and 2.20 and 1.12 KHz for low frequency limit estimates depending on the equation used. Results obtained here for *Protungulatum* are congruent with these values.

Regardless of hearing limit estimates, the secondary bony lamina of AMNH-VP 118359 covers 61 % of the length of the cochlear canal. The presence of this structure implies a narrow laminar gap (distance between the primary and secondary bony laminae) and suggests a narrow basilar membrane, which is most suitable for high-frequency hearing (Manley 1971, 1972). The laminar gap continuously and gradually increases from the base to the apex of the cochlear canal in AMNH-VP 118359 (see online supplementary material Fig. O1). Small differences in basal and apical dimensions of the basilar membrane have been reported to correspond to a narrow frequency range (Ketten 1992; Ketten et al. 1992). The relatively small width gradients of AMNH-VP 118359 along most of the cochlear canal length suggest that the range of frequencies encoded was probably narrow. This conclusion corresponds to that of Meng and Fox (1995) for the placental inner ears from Bug Creek Anthills and is congruent with the hearing limit range estimates calculated above.

Protungulatum was a small sized mammal with a body mass ranging from 148.4 g in *Protungulatum gorgun* to 225.8 g in *Protungulatum donnae* (Wilson 2013), which would have put the genus close in size to that of a tree squirrel. Mammals with small heads and close-set ears are often better able to hear high-frequency sounds because of short interaural distance (Heffner and Heffner 1992, 2008). The estimated body mass for *Protungulatum* is congruent with a high range of audible frequencies. High-frequency hearing has been proposed as a primitive trait among therian mammals (e.g., Ravizza et al. 1969a, 1969b). The extension of the secondary bony lamina of *Protungulatum* along the cochlear canal is important compared to the early euungulates *Diacodexis ilicis* and *Hyopsodus lepidus*; but it is also greater than that of Mesozoic non-placental eutherians when expressed as a percentage of the total coiling (Table 1). Whether *Protungulatum* had even greater specialization for high frequency hearing within placental therians, requires further testing.

Discussion

Noteworthy Morphological Similarities and Differences within Eutherians

According to the recent parsimony analysis of O'Leary et al. (2013) combining both molecular and phenomic data in a large sample of characters and taxa across Mammalia, *Protungulatum* is the most basal member of Pan-Euungulata, and along with a number of other early Tertiary fossils is among the stem taxa to Euungulata, a crown clade that

includes both Artiodactyla and Perissodactyla (see also Asher et al. 2009). This result corroborates earlier suggestions by Zack et al. (2005), but it contrasts those of Wible et al. (2007, 2009), which included fewer characters (including no gene data) but a more dense sampling of non-placental eutherians. Those studies suggested that *Protungulatum* was phylogenetically outside Placentalia. The recent results of Muizon et al. (2015) found *Protungulatum* within Laurasiatheria a result more congruent with O'Leary et al. (2013).

Inner ear characters have not been studied extensively in a phylogenetic context and were not a large part of the O'Leary et al. (2013) paper because the data are hard to obtain and remain scarce in the literature. The inner ear of *Protungulatum* mostly exhibits characters that have been considered primitive for both Theria and Eutheria, either based on outgroup comparison criteria (Ketten 1992; Meng and Fox 1995), or on ancestral state reconstruction (Ekdale 2009, 2013). These include: 1) a cochlea with few coils and short length (Meng and Fox 1995); 2) the presence of the secondary spiral lamina (Ketten 1992; Meng and Fox 1995);3) a secondary common crus (Ekdale 2009, 2013); 4) a plane of the lateral semicircular canal positioned low with respect to the ampullar entrance of the posterior semicircular canal (Ekdale 2009, 2013); 5) a low aspect ratio of the cochlea (Ekdale 2009, 2013); and 6) the small fibers of the cochlear nerve passing through numerous tubules in the modiolus in a radial fashion (Meng and Fox 1995). Lack of a secondary common crus is the single unambiguous synapomorphy of the inner ear proposed for Placentalia according to the analysis of Ekdale (2013). The presence of this structure in several stem representatives of clades within Placentalia (e.g., Euungulata, Ravel and Orliac 2015; Afrotheria, Benoit et al. 2013; Litopterna, Billet et al. 2015), that were not part of Ekdale's (2013) analyses, however, suggests that this feature shows high homoplasy and should perhaps be investigated in the context of a broad taxonomic and character sample. In addition to these symplesiomorphic characters at the level of Theria, the inner ear of *Protungulatum* is strikingly similar to that of non-placental Mesozoic eutherians by the orientation of the common crus axis that is not orthogonal to the line of the dorsal edge of the vestibule (Fig. 3a-c vs. 3e). Such an inclination of the common crus is, to our knowledge, not observed in extant representatives of Placentalia.

The inner ear of *Protungulatum* differs from non-placental Late Cretaceous eutherian mammals such as *Kulbekia*, *Ukhaatherium*, and zhelestids by the orientation of the axis of the cochlea: the angle formed by the planes of the first turn of the cochlea and the LSC is more open in *Protungulatum* than in Late Cretaceous eutherian mammals (as figured by Ekdale 2009, 2013) and is closer to the configuration observed in *Hyopsodus lepidus* and *Diacodexis ilicis* (Fig. 3). However, the inner ear of *Protungulatum* differs morphologically from the latter two taxa by most of the characters cited above in having: 1) a much lower coiling of the cochlea (Table 1) and a lower cochlear ratio; 2) a longer extension of the secondary bony lamina; and 3) an "inclined" common crus relative to the dorsal edge line of the vestibule. In addition to these characters, *Protungulatum* also differs from *D. ilicis* by a having a vestibular aqueduct originating lateral to the root of the common crus, and from *H. Lepidus* and *D. ilicis* by the presence of a marked cochlear fossula, accompanied by a horseshoe shaped pocket located close to the cochlear aqueduct base. Thus, based on inner ear morphology, *Protungulatum* shares only a few characters with euungulate taxa and is morphologically closer to the symplesiomorphic morphology of non-placental Late Cretaceous eutherian mammals.

The recently published inner ear of the early Paleocene pantodont *Alcidedorbignya inopinata*, a taxon discovered to be nested within Laurasiatheria (Muizon et al. 2015), shows several character states common to *Protungulatum*. These species share a low coiling of the cochlea (*Alcidedorbignya* number of cochlear turn =1.5, Muizon et al. 2015: table 5), a long distance separating the basis of the common crus and the anterior ampulla (Muizon et al. 2015: fig. 52C, D), the presence of a cochlear fossula (Muizon et al. 2015: fig. 52A, C), a widely open angle between the planes of the first turn of the cochlea and the LSC (for *Alcidedorbignya* see Muizon et al. 2015: fig. 52C), and a vestibular aqueduct origin slightly anterior to the common crus basis. Contrary to *Protungulatum*, the common crus axis of *Alcidedorbignya* is orthogonal to the line of the dorsal edge of the vestibule (Muizon et al. 2015: fig. 52E).

Recent results of molecular phylogeny have placed South American ungulates, including a subfossil representative of Litopterna (*Macrauchenia*), as sister taxa to crown Perissodactyla (Buckley 2015; Welker et al. 2015), within Euungulata. The bony labyrinth of *Protungulatum* is morphologically close to that of late Palaeocene/early Eocene litopterns from Itaboraí (Fig. 3), sharing with them a close trajectory of the spiral mordiolar vein and close inner structures of the modiolus, presence of the horseshoe shaped structure on the dorsal part of the fossula, and an inflated base of the vestibular aqueduct distinct from common crus. Still not enough data are available to properly discuss how these characters are distributed within Placentalia in general and Laurasiatheria in particular.

Conclusions

The bony labyrinth of *Protungulatum* shows a distinctive morphology with a posterior inclination of the axis of the common crus, so that it is not orthogonal to the line of the dorsal edge of the vestibule, and a weakly coiled cochlea with a low aspect ratio and a long secondary spiral lamina (running

over 61 % of the length of the short cochlear canal). The fenestra cochleae is joined externally by a wide cochlear fossula, the external opening of which is smaller than the diameter of the fenestra cochleae. The dorsal part of the fossula bears a horseshoe shaped structure that connects to the root of the cochlear aqueduct. Reconstruction of the innervation and vasculature of the cochlea of *Protungulatum* permitted visualization of channels made by the small fibers of the cochlear nerve passing through the numerous tubules of the modiolus and the primary bony lamina in a radial fashion, as well as the spiral modiolar artery and vein. The spiral modiolar vein was located at the periphery of the cochlear canal and left grooves in the outer wall of the cochear canal, with a distinct canal for the vena aquaeductus cochleae, parallel to the cochlear aqueduct. Estimation of the auditory capability of *Protungulatum* based on cochlear morphology indicates that *Protungulatum* was specialized for high-frequency hearing, with estimated low frequency limits above 1 KHz.

The bony labyrinth of *Protungulatum* is markedly different from that of the pan-euungulate *Hyopsodus* and of the pan-artiodactyl *Diacodexis* in retaining characters of the cochlea previously considered to be plesiomorphic at the level of Theria and Eutheria but that are no longer present in *Hyopsodus* and *Diacodexis*. These are a cochlea with few coils and short length, and very low aspect ratio. The presence of a secondary bony lamina, of a secondary common crus, of a plane of the lateral canal positioned low with respect to the ampullar entrance of the posterior canal are other characters considered as symplesiomorphic at the level of Eutheria (Ekdale 2013), but they are also observed in early pan-euungulates. In addition to these plesiomorphic characters, *Protungulatum* shares with Late Cretaceous non-placental eutherians, *Kulbeckia* and *Ukhaatherium*, the posterior orientation of the common crus. Late Cretaceous non-placental eutherians also show an outpocketing of the cochlear fossula at the basis of the cochlear aqueduct, but it is larger and not horseshoe shaped. *Protungulatum* shares with pan-euungulate placental taxa an open angle formed by the planes of the first turn of the cochlea and the LSC. It further shares with South American litoptern from Itaboraí (Brazil) a vestibular aqueduct originating slightly anterior to the common crus base, the presence of a cochlear fossula extending dorsally in a horseshoe shaped diverticulum (not observed in *Hyopsodus* and *Diacodexis*), and irrigation of the cochlea (spiral modiolar vein) located at the periphery of the cochlear canal, with distinct canal for the vena aquaeductus cochleae. *Protungulatum* also shares with the early Paleocene pantodont *Alcidedorbignya* a mixture of characters, some being also present in Late Cretaceous non-placental eutherians (a low coiling of the cochlea), others present in Laurasiatheria (a widely open angle between the planes of the first turn of the cochlea and the LSC), others in litoptern and notoungulate (presence of a cochlear fossula, vestibular aqueduct originating slightly anterior to the common crus base). The phylogenetic importance and evolutionary history of these characters have to be tested through a formal phylogenetic analysis, with additional inner ear data from other early placental mammal taxa.

Acknowledgments For access to the micro CT-scanner we thank S. Judex and S. Xu of the Department of Biomedical Engineering, Stony Brook University, New York. We are also grateful to G. Billet for providing us with supplemental images of the bony labyrinth of the litoptern from Itaboraí and for his thorough review of the manuscript. This is ISEM publication n° ISEM 2016-017. This research was supported by grants NSF-DEB 0629836, 9903964, NSF BDI-0743309, NSF-EAR 0622359 to M. A. O.

Appendix

Table 2 Alphabetical list of anatomical terms used. Source is Giannini et al. (2006) unless otherwise specified; synonyms are noted in some cases. Terminology generally follows the Nomina Anatomica Veterinaria (NAV) as applied by Giannini et al. (2006) and Wible (2003), who listed standardized cranial anatomical terms in English for many Latin Nomina Anatomica Veterinaria terms and synonymized many terms

Term	Sources other than Giannini et al. (2006)
Ampulla	NAV
Ampular branche of vestibulo-cochlear nerve	NAV, N. ampullaris posterior
Anterior ampulla	NAV
Anterior semicircular canals	NAV
Area cribrosa media	NAV
Area cribrosa superior	NAV
Area vestibularis media	NAV
Area vestibularis superior	NAV
Basilar membrane	NAV, lamina baislaris
Bony labyrinth	NAV, labyrinthus osseus
Cochlea	NAV
Cochlear aqueduct	Sisson 1911, canaliculus cochleae
Cochlear canal	NAV, canalis spiralis cochleae
Cochlear fossula	Bast and Anson 1952, fossula fenestra cochleae
Common crus	crus commune; NAV, crus osseum commune
Cribriform plate of the modiolus	NAV, tractus spiralis foraminosus
Elliptical recess	NAV, recessus ellipticus
Endolymphatic duct	NAV, Ductus endolymphaticus
External aperture of cochlear fossula	Billet and Muizon 2013
Facial nerve	
Fenestra cochleae	

Table 2 (continued)

Term	Sources other than Giannini et al. (2006)
Fenestra vestibuli	
Foramen acusticum inferius	
Foramen acusticum superius	
Foramen singulare	NAV
Helicotrema	NAV
Internal acoustic meatus	
Laminar gap	Ekdale and Rowe 2011
Lateral ampulla	NAV
Lateral semicircular canals	NAV
Mastoid region	McDowell 1958; MacPhee 1981
Modiolus	NAV
Organ of Corti	Echteler et al. 1994
Pars canalicularis	
Pars cochlearis	
Perilymphatic duct	NAV, ductus perilymphaticus
Petrosal	
Posterior ampulla	NAV
Posterior semicircular canals	NAV
Primary bony lamina	NAV, lamina spiralis ossea
Promontorium	
Saccular branch of vestibulocochlear nerve	NAV, N. sacccularis
Saccule	NAV, sacculus
Scala tympani	NAV
Scala vestibuli	NAV
Secondary bony lamina	NAV, lamina spiralis secundaria
Secondary common crus	Ekdale 2009
Secondary tympanic membrane	NAV, membrana tympani secundaria
Semicircular canals	NAV
Spherical recess	NAV, recessus sphericus
Spiral canal	NAV, canalis spiralis modioli
Spiral ganglion	NAV, ganglion spirale cochleae
Spiral modiolar artery	NAV, arteria labyrinthi Ramus cochlearis
Spiral modiolar vein	vena spiralis modioli, Schaller 1992
Subarcuate fossa	
Utricular branch of vestibulocochlear nerve	NAV, N. utricularis
Utricule	NAV, utriculus
Vena aquaeductus cochleae	Frick et al. 1992; Feneis 1993
Vena vestibularis	NAV, Vv. vestibulares
Vestibular aqueduct	NAV, aqueductus vestibuli
Vestibule	NAV, vestibulum
Vestibulocochlear nerve	NAV, N. vestibulocochlearis

References

Asher RJ, Bennett N, Lehmann T (2009) The new framework for understanding placental mammal evolution. Bioessays 31(8):853–864. doi:10.1002/bies.200900053

Axelsson A, Ryan AF (1988) Circulation of the inner ear: I. Comparative study of the vascular anatomy in the mammalian cochlea. In: Jahn AF, Santos-Sacchi J (eds) Physiology of the Ear. Taylor & Francis, US, pp 295–316

Barone R, Bortolami R (2004) Moelle épiniere. Neurologie I—systeme nerveux central, Tome 6. Vigot Frères, Paris

Bast TH, Anson BJ (1952) The development of the cochear fenestra, fossula and secondary tympanic membrane. Q Bull Northwest Univ Med Sch 26(4):344–373

Benoit J, Orliac MJ, Tabuce R (2013) The petrosal of the earliest elephant-shrew *Chambius* (Macroscelidea: Afrotheria) from the Eocene of Djebel Chambi (Tunisia) and the evolution of middle and inner ear of elephant-shrews. J Syst Palaeontol 11(8):907–923. doi:10.1080/14772019.2012.713400

Billet G, Muizon C de (2013) External and internal anatomy of a petrosal from the late Paleocene of Itaboraí, Brazil, referred to Notoungulata (Placentalia). J Vertebr Paleontol 33(2):455–469. doi:10.1080/02724634.2013.722153

Billet G, Hautier L, Asher RJ, Schwarz C, Crumpton N, Martin T, Ruf I (2012) High morphological variation of vestibular system accompanies slow and infrequent locomotion in three-toed sloths. Proc Roy Soc Lond B 279:3932–3939. doi:10.1098/rspb.2012.1212

Billet G, Muizon C de, Schellhorn R, Ruf I, Ladevèze S, Bergqvist L (2015) Petrosal and inner ear anatomy and allometry amongst specimens referred to Litopterna (Placentalia). Zool J Linn Soc 173(4):956–987. doi:10.1111/zoj.12219

Buckley M (2015) Ancient collagen reveals evolutionary history of the endemic South American 'ungulates.' Proc Roy Soc Lond B 282(1806):20142671. doi:10.1098/rspb.2014.2671

Cifelli RL (1982) The petrosal structure of *Hyopsodus* with respect to that of some other ungulates, and its phylogenetic implications. J Paleontol 56(3):795–805

Danilo L (2012) Evolution des structures neurocrâniennes des Equoidea (Perissodactyla, Mammalia) européens paléogènes. Université de Montpellier, Unpublished Thesis

Danilo L, Remy J, Vianey-Liaud M, Mérigeaud S, Lihoreau F (2015). Intraspecific variation of endocranial structures in extant *Equus*: a prelude to endocranial studies in fossil equoids. J Mammal Evol 22(4):561–582

Echteler SM, Fay RR, Popper AN (1994) Structure of the mammalian cochlea. In: Fay RR, Popper AN (eds) Comparative Hearing: Mammals. Springer-Verlag, New York, pp 134–171

Ekdale EG (2009) Variation within the bony labyrinth of mammals. Dissertation, The University of Texas

Ekdale EG (2010) Ontogenetic variation in the bony labyrinth of *Monodelphis domestica* (Mammalia: Marsupialia) following ossification of the inner ear cavities. Anat Rec 293:1896–1912

Ekdale EG (2013) Comparative anatomy of the bony labyrinth (inner ear) of placental mammals. PloS ONE 8(6):1–100. doi:10.1371/journal.pone.0066624

Ekdale EG, Racicot RA (2015) Anatomical evidence for low frequency sensitivity in an archaeocete whale: comparison of the inner ear of *Zygorhiza kochii* with that of crown Mysticeti. J Anat 226(1):22–39

Ekdale EG, Rowe T (2011) Morphology and variation within the bony labyrinth of zhelestids (Mammalia, Eutheria) and other therian mammals. J Vertebr Paleontol 31(3):658–675. doi:10.1080/02724634.2011.557284

Ekdale EG, Archibald JD, Averianov AO (2004). Petrosal bones of placental mammals from the Late Cretaceous of Uzbekistan. Acta Palaeontol Polonica 49(1):161–176

Feneis H (1993) Anatomisches Bildwörterbuch der lnternationales Nomenklatur, 7th edn. Georg Thieme Verlag, Stuttgart

Fleischer G (1973) Studien am Skelett des Gehörorgans der Saügetiere, einschließlich des Menschen. Saügetierk Mitt 21:131–239

Fleischer G (1976) Hearing in extinct cetaceans as determined by cochlear structure. J Paleontol: 133–152

Frick H, Leonhardt H, Starck D (1992) Spezielle Anatomie (Vol. 2). Georg Thieme Verlag, Stuttgart

Geisler JH, Luo Z (1996). The petrosal and inner ear of *Herpetocetus* sp. (Mammalia: Cetacea) and their implications for the phylogeny and hearing of archaic mysticetes. J Paleontol 70(6):1045–1066.

Giannini NP, Wible JR, Simmons NB (2006) On the cranial osteology of *Chiroptera. I. Pteropus* (Megachiroptera, Pteropodidae). Bull Am Mus Nat Hist 295:1–134

Gray AA (1908) The Labyrinth of Animals: including Mammals, Birds, Reptiles and Amphibians (Vol. 2). J and A Churchill, London

Gray H (1918) Henry Gray's Anatomy of the Human Body. Lea and Febiger, Philadelphia

Heffner RS, Heffner HE (1992). Evolution of sound localization in mammals. In: Webster DB, Fay RR, Popper AN (eds) The Evolutionary Biology of Hearing. Springer, New York, pp 691–715

Heffner RS, Heffner HE (2008) High-frequency hearing. In: Dallos P, Oertel D, Hoy R (eds) Handbook of the Senses: Audition. Elsevier, New York, pp. 55–60

Ketten DR (1992) The cetacean ear: form, frequency, and evolution. In: Thomas J, Kastelein RA, Supin AY (eds) Marine Mammal Sensory Systems. Plenum Press, New York, pp 53–75

Ketten DR, Odell DK, Domning DP (1992) Structure, function, and adaptation of the manatee ear. In: Kastelein RA, Supin AYa, Thomas JA (eds) Marine Mammal Sensory Systems. Plenum Press, New York, pp 77–95

Lebrun R (2014) ISE-MeshTools, a 3D interactive fossil reconstruction freeware. 12th Annual Meeting of EAVP, Torino, Italy

Lebrun R, De León MP, Tafforeau P, Zollikofer C (2010). Deep evolutionary roots of strepsirrhine primate labyrinthine morphology. J Anat 216(3):368–380

Lewis ER, Leverenz EL, Bialek WS (1985) The Vertebrate Inner Ear. CRC Press Llc, Boca Raton

MacIntyre GT (1972) The trisulcate petrosal pattern of mammals. In: Dobzhansky T, Hecht M, Steere WC (eds) Evolutionary Biology, Vol. 6. Appleton-Century-Crofts, New York, pp 275–303

MacPhee RD (1981) Auditory regions of primates and eutherian insectivores: morphology, ontogeny, and character analysis. Contrib Primatol 18:1–282

MacPhee RDE (1994) Morphology, adaptations, and relationships of *Plesiorycteropus*, and a diagnosis of a new order of eutherian mammals. Bull Am Mus Nat Hist 220:1–214

Macrini TE, Flynn JJ, Croft DA, Wyss AR (2010) Inner ear of a notoungulate placental mammal: anatomical description and examination of potentially phylogenetically informative characters. J Anat 216(5):600–610

Macrini TE, Flynn JJ, Ni X, Croft DA, Wyss AR (2013). Comparative study of notoungulate (Placentalia, Mammalia) bony labyrinths and new phylogenetically informative inner ear characters. J Anat 223(5):442–461

Manley GA (1971) Some aspects of the evolution of hearing in vertebrates. Nature 230:506–509. doi:10.1038/230506a0

Manley GA (1972) A review of some current concepts of the functional evolution of the ear in terrestrial vertebrates. Evolution 26(4):608–621. doi:10.2307/2407057

Manoussaki D, Chadwick RS, Ketten DR, Arruda J, Dimitriadis EK, O'Malley JT (2008) The influence of cochlear shape on low-frequency hearing. Proc Natl Acad Sci USA 105:6162–6166

McDowell SB Jr (1958) The Greater Antillean insectivores. Bull Am Mus Nat Hist 115:117–214

Meng J, Fox RC (1995) Osseous inner ear structures and hearing in early marsupials and placentals. Zool J Linn Soc 115(1):47–71. doi:10.1006/zjls.1995.0033

Muizon C de, Billet G, Argot C, Ladevèze S, Goussard F (2015) *Alcidedorbignya inopinata*, a basal pantodont (Placentalia, Mammalia) from the early Palaeocene of Bolivia: anatomy, phylogeny and palaeobiology. Geodiversitas 37(4):397–634

Novacek MJ (1986) The skull of leptictid insectivorans and the higher-level classification of eutherian mammals. Bull Am Mus Nat Hist 183:1–112

O'Leary MA (2010). An anatomical and phylogenetic study of the osteology of the petrosal of extant and extinct artiodactylans (Mammalia) and relatives. Bull Am Mus Nat Hist 335:1–206. doi:10.1206/335.1

O'Leary MA, Bloch JI, Flynn JJ, Gaudin TJ, Giallombardo A, Giannini NP, Goldberg SL, Kraatz BP, Luo ZX, Meng J, Ni X, Novacek MJ, Perini FA, Randall ZS, Rougier RW, Sargis EJ, Silcox MT, Simmons NB, Spaulding M, Velazco PM, Weksler M, Wible JR, Cirranello A (2013) The placental mammal ancestor and the post-K-Pg radiation of placentals. Science 6120(339):662–667. doi:10.1126/science.1229237

Orliac MJ (2013) The petrosal bone of extinct Suoidea (Mammalia, Artiodactyla). J Syst Paleontol 11(8):925–945. doi:10.1080/14772019.2012.704409

Orliac MJ, Benoit J, O'Leary MA (2012) The inner ear of *Diacodexis*, the oldest artiodactyl mammal. J Anat 221:417–426. doi:10.1111/j.1469-7580.2012.01562.x

Orliac MJ, O'Leary M (2011) Endocranial structures of *Diacodexis* (Mammalia, Artiodatyla). J Vertebr Paleontol 31(suppl. to no 3):169

Orliac MJ, O'Leary MA (2014) Comparative anatomy of the petrosal bone of dichobunoids, early members of Artiodactylamorpha (Mammalia). J Mammal Evol 21(3):299–320

Ravel A, Orliac MJ (2015) The inner ear morphology of the 'condylarthran' *Hyopsodus lepidus*. Hist Biol 27(8):957–963. doi:10.1080/08912963.2014.915823

Ravizza RJ, Heffner HE, Masterton B (1969a) Hearing in primitive mammals, I: Opossum (*Didelphis virginianus*). J Aud Res 9:1–7

Ravizza RJ, Heffner HE, Masterton B (1969b) Hearing in primitive mammals: II. Hedgehog (*Hemiechinus auritus*). J Aud Res 9:8–11

Rosowski JJ (1992) Hearing in transitional mammals: predictions from the middle-ear anatomy and hearing capabilities of extant mammals. In: Webster DB, Popper AN, Fay RR (eds) The Evolutionary Biology of Hearing. Springer, New York, pp 615–631

Rosowski JJ, Graybeal A (1991) What did *Morganucodon* hear? Zool J Linn Soc 101(2):131–168. doi:10.1111/j.1096-3642.1991.tb00890.x

Rougier GW, Wible JR (2006) Major changes in the ear region and basicranium of early mammals. In: Carrano MT, Gaudin TJ, Blob RW, Wible JR (eds) Amniote Paleobiology: Phylogenetic and Functional Perspectives on the Evolution of Mammals, Birds, and Reptiles. The University of Chicago Press, Chicago, pp 269–311

Schaller O, Constantinescu GM, Habel RE, Sack WO, Simoens P, De Vos NR (1992) Illustrated Veterinary Anatomical Nomenclature. Ferdinand Enke Verlag, Stuttgart

Sloan RE, Van Valen L (1965) Cretaceous mammals from Montana. Science 148(3667):220–227. doi:10.1126/science.148.3667.220

Smit J, Van der Kaars S (1984) Terminal Cretaceous extinctions in the Hell Creek area, Montana: compatible with catastrophic extinction. Science 223(4641):1177–1179

Spoor F, Garland T, Krovitz G, Ryan TM, Silcox MT, Walker A (2007) The primate semicircular canal system and locomotion. Proc Natl Acad Sci USA 104:10808–10812. doi:10.1073/pnas.0704250104

Spoor F, Zonneveld F (1998) Comparative review of the human bony labyrinth. Yearb Phys Anthropol 41:211–251

Welker F, Collins MJ, Thomas JA, Wadsley M, Brace S, Cappellini E, Turvey TS, Reguero M, Gelfo JN, Kramarz A, Burger J, Thomas-

Oates J, Ashford DA, Ashton PD, Rowsell K, Porter DM, Kessler B, Fischer R, Baessmann C, Kaspar S, Olsen JV, Kiley P, Elliott JA, Kelstrup CD, Mullin V, Hofreiter M, Willerslev E, Hublin J-J, Orlando L, Barnes I, MacPhee RDE (2015) Ancient proteins resolve the evolutionary history of Darwin's South American ungulates. Nature 522:81–84. doi:10.1038/nature14249

West CD (1985) The relationship of the spiral turns of the cochlea and the length of the basilar membrane to the range of audible frequencies in ground dwelling mammals. J Acoust Soc Am 77:1091–1101. doi:10.1121/1.392227

Wible JR (1990) Petrosals of Late Cretaceous marsupials from North America, and a cladistic analysis of the petrosal in therian mammals. J Vertebr Paleontol 10:183–205

Wible JR (2003) On the cranial osteology of the short-tailed opossum *Monodelphis brevicaudata* (Didelphidae, Marsupialia). Ann Carnegie Mus 72(3):137–202

Wible JR (2010) Petrosal anatomy of the nine-banded armadillo, *Dasypus novemcinctus* Linneaus, 1758 (Mammalia, Xenarthra, Dasypodidae). Ann Carnegie Mus 79(1):1–28. doi:10.2992/007.079.0101

Wible JR, Rougier GW, Novacek MJ, Asher RJ (2009) The Eutherian mammal *Maelestes gobiensis* from the Later Cretaceous of Mongolia and the phylogeny of Cretaceous Eutheria. Bull Am Mus Nat Hist 327:1–123. doi:10.1206/623.1

Wible JR, Rougier GW, Novacek MJ, McKenna MC (2001) Earliest eutherian ear region: a petrosal referred to *Prokennalestes* from the Early Cretaceous of Mongolia. Am Mus Novitates 3322:1–44

Wible JR, Rougier GW, Novacek MJ, McKenna MC, Dashzeveg D (1995) A mammalian petrosal from the Early Cretaceous of Mongolia: implications for the evolution of the ear and mammaliamorph interrelationships. Am Mus Novitates 3149:1–19

Wible JR, Wang Y, Li C, Dawson M (2007) Cranial anatomy and relationships of a new ctenodactyloid (Mammalia, Rodentia) from the early Eocene of Hubei Province, China. Ann Carnegie Mus 74(2):91–150

Wilson GP (2013) Mammals across the K/Pg boundary in northeastern Montana, USA: dental morphology and body-size patterns reveal extinction selectivity and immigrant-fueled ecospace filling. Paleobiology 39(3):429–469. doi:10.1666/12041

Zack S, Penkrot TA, Bloch JI, Rose KD (2005) Affinities of 'hyopsodontids' to elephant shrews and a Holarctic origin of Afrotheria. Nature 434:497–501. doi:10.1038/nature03351